Pramana – J. Phys. (2022) 96:227
https://doi.org/10.1007/s12043-022-02472-2

Dynamics analysis in a non-smooth Lü system with two time scales

MIAO PENG

School of Mathematical Sciences, Jiangsu University, Zhenjiang 212013, China
E-mail: pengmiao@ujs.edu.cn

MS received 8 May 2022; revised 15 June 2022; accepted 1 August 2022

Abstract. To explore the bursting behaviours in a dynamic system with non-smooth factor, this paper takes Lü system as an example, introduces a non-smooth term and a periodic external excitation, ensures that there exists an order gap between the natural frequency and the exited frequency, then a non-smooth dynamic system with two time scales is established. Through the stability analysis of the equilibrium point, the conditions of fold bifurcation and Hopf bifurcation are given. The numerical simulations show the bursting oscillations of the system under different parameter values and the dynamic behaviours of the trajectory at the non-smooth interface. In addition, combining with numerical calculation and related bifurcation theory, the bifurcation types of the system at the interface are determined. Finally, the mechanism of oscillations is revealed by the superposition of bifurcation curves and transformed phase portraits.

Keywords. Non-smooth; two time scales; stability; bifurcation; bursting oscillations.

PACS Nos 05.45.-a; 05.45.Pq; 05.45.Xt

1. Introduction

In recent years, the complexity research of coupled systems with different time scales, as one of the hot topics, not only has important theoretical significance, but also has an extensive natural and engineering background. Transmission tower line system is a typical example of multi-time scale coupled system. Due to the qualitative differences in stiffness and flexibility between transmission tower and transmission line, the system will have behaviours and interaction on different time scales. Through its dynamic analysis, the design level of transmission tower line system can be improved, and its ability to resist the disastrous damage of earthquake and environmental load can also be enhanced [1]. In addition, this factor is involved in many dynamic systems in physics [2], chemistry [3], biology [4,5] and engineering [6,7].

Generally, nonlinear systems under multi-scale coupling can often show complex dynamic characteristics such as mixed-mode oscillations (also known as bursting oscillations). The characteristics of mixed-mode oscillations are that the alternation of relatively large-amplitude oscillations and small-amplitude oscillations can be observed in the evolution process of each period [8,9]. When the state variable is in large-amplitude oscillations, it is called the spiking states (SPs). When it is in small-amplitude oscillations, it corresponds to the quiescent states (QSs). The above described oscillations appear when the trajectory of the system oscillates back and forth between SPs and QSs. The aforesaid phenomena were first found in the early research on Van der pol equation. It was in 1963 that Hodgkin and Huxley established a neuron discharge model with two time scales [10], that is, the famous H-H model. And after successfully reproducing the bursting of neurons, the coupling problem of different time scales has attracted the attention of scholars at home and abroad. However, due to the lack of effective theoretical analysis methods at that time, relevant research mainly focussed on approximate solutions such as singular perturbation methods, experimental analysis, numerical simulation, etc. [11,12]. In 2000, Izhikevich [13] introduced the fast–slow analysis method of Rinzel [14], and the numerical solution of relevant discussion is promoted to the level of mechanism analysis. The core idea is to dissect the coupling system on different time scales, and then discuss the interaction between different scales [15]. In view of this method, some scholars have carried out a series of work on the generation mechanism of bursting behaviours

Published online: 28 November 2022

of systems with two time scales. For example, Izhikevich [13] summarised various bursting phenomena and codimension-one bifurcation mechanisms. Brøns *et al* [16] established a three-dimensional forest pest model with two time scales and discussed the bursting oscillations caused by singular Hopf bifurcation. Zhang *et al* [17] studied the generation mechanism of different bursting behaviours and the transition process between different bursting behaviours by introducing periodic excitation term into Lü system. Xing *et al* [18] explored the symmetric bursting oscillations and bifurcation mechanism of controlled Lorenz system with periodic excitation.

Recently, there have been some achievements on the problem of multi-time scale coupling, but most of the work is developed around smooth systems. In fact, there exist non-smooth factors in practical engineering system, for example, the switch in the circuit [19], the collision, dry friction in the mechanical system [20,21], etc. Similarly, the non-smooth characteristics are everywhere in the fields of nature and humanities, such as threshold harvesting strategy in biology [22], modelling of snake robot [23], energy markets economy [24], model of sustainable development [25], etc. Due to the influence of this factor, the related systems will lead to richer dynamic behaviours. It is necessary to carry out further exploration in future.

Lorenz first put forward a chaotic model in 1963. Then, chaotic attractors first appeared in the public view. Subsequently, Lv and Chen proposed Lü system at the beginning of 21st century [26]. The discovery of this system constituted a complete Lorenz system family, which greatly expanded the scope of the whole Lorenz system, and Lü system can be transformed between Lorenz and Chen systems. Therefore, Lü system is favoured by many scholars. In recent years, although the knowledge related to the characteristics, control and synchronisation of Lü system are gradually enriched, most studies still explore the single time scale [27–29], and there are few studies about the dynamic behaviours of system under the multi-time scale [17,30].

Based on the above discussions, here Lü system is selected as an example. By considering a periodic external excitation and a non-smooth factor, the dynamic evolution process of non-smooth system with parameter changes under two time scales is investigated. The paper is organised as follows. In §2, the mathematical model is presented. In §3, the corresponding bifurcation analysis is studied. By applying fast–slow analysis method, as well as combining with transformed phase portraits, the dynamical mechanism of two different cases of bursting is revealed. Finally, a brief summary of this paper is given.

2. Mathematical model

The mathematical model of the Lü system is as follows:

$$\begin{cases} \dfrac{\mathrm{d}x}{\mathrm{d}t} = a(y-x), \\ \dfrac{\mathrm{d}y}{\mathrm{d}t} = -xz + cy, \\ \dfrac{\mathrm{d}z}{\mathrm{d}t} = xy - bz. \end{cases} \tag{1}$$

where $a, b > 0, c \in R$. From the first equation in system (1), it is known that the system is symmetrical about the z-axis, that is, the vector field has invariance about transformation $(x, y, z) \to (-x, -y, z)$. The equilibrium point of the system can be expressed as $E_{\pm}(\pm\sqrt{bc}, \pm\sqrt{bc}, c)$. To explore the dynamic behaviours in system (1) under the influence of two time scales and non-smooth factor, the Lü system is used, by adding external periodic excitation and non-smooth factor, and the new mathematical model can be described in the following form:

$$\begin{cases} \dfrac{\mathrm{d}x}{\mathrm{d}t} = a(y-x), \\ \dfrac{\mathrm{d}y}{\mathrm{d}t} = -xz + cy + a_0 \ \mathrm{sgn}\ y + A\cos(\omega t), \\ \dfrac{\mathrm{d}z}{\mathrm{d}t} = xy - bz, \end{cases} \tag{2}$$

where a, b, c and a_0 are constants, and a, b, c are greater than 0, $\mathrm{sgn}\, y$ is a symbolic function. Here, variable $w = A\cos(\omega t)$ is defined as external periodic excitation term. A and ω represent the amplitude and frequency of external periodic excitation, respectively. When the natural frequency ω_0 is close to the exciting frequency ω, the vector field will produce resonance phenomenon. When an order gap exists between the two frequencies, the influence of two time scales may occur, which often show bursting oscillations. Using the fast–slow analysis method, the external periodic excitation term is regarded as a whole and set as the parameter w. System (2) can be shown as follows:

$$\begin{cases} \dfrac{\mathrm{d}x}{\mathrm{d}t} = a(y-x), \\ \dfrac{\mathrm{d}y}{\mathrm{d}t} = -xz + cy + a_0 \ \mathrm{sgn}\ y + w, \\ \dfrac{\mathrm{d}z}{\mathrm{d}t} = xy - bz. \end{cases} \tag{3}$$

Compared with system (2), the above system with fast–slow parameters are defined as generalised autonomous system, and its corresponding equilibrium point is called the generalised equilibrium point. System (3) can also

be defined as fast subsystem relative to parameter w. Obviously, after such a transformation of the original system, not only the influence of period excitation can be analysed but also the fast–slow analysis method can be utilised to study its dynamic behaviours and formation mechanism. Moreover, owing to the existence of non-smooth factor, the dynamic behaviours of system at non-smooth interface will become more abundant.

3. Bifurcation analysis

Due to the existence of non-smooth interface $\Sigma = \{(x, y, z)|y = 0\}$, the vector field of the system is divided into two smooth regions, $D_+ = \{(x, y, z)|y > 0\}$ and $D_- = \{(x, y, z)|y < 0\}$, respectively, corresponding to two different smooth subsystems:

When $y > 0$,

$$\dot{X} = F_+(X) = \begin{cases} \dfrac{\mathrm{d}x}{\mathrm{d}t} = a(y - x), \\ \dfrac{\mathrm{d}y}{\mathrm{d}t} = -xz + cy + a_0 + w, \\ \dfrac{\mathrm{d}z}{\mathrm{d}t} = xy - bz. \end{cases} \tag{4}$$

When $y < 0$,

$$\dot{X} = F_-(X) = \begin{cases} \dfrac{\mathrm{d}x}{\mathrm{d}t} = a(y - x), \\ \dfrac{\mathrm{d}y}{\mathrm{d}t} = -xz + cy - a_0 + w, \\ \dfrac{\mathrm{d}z}{\mathrm{d}t} = xy - bz. \end{cases} \tag{5}$$

The characteristic equation of the system can be written as

$$\begin{aligned} F(\lambda) = {} & \lambda^3 + (b - a - c)\lambda^2 \\ & + (-ab - za - cb + x^2 + ac)\lambda \\ & + acd - ax^2 - zab - yax. \end{aligned} \tag{6}$$

Next, the focus is on the equilibria of two subsystems. By calculation, it is concluded that their generalised equilibrium point is $(y, y, \frac{y^2}{b})$, where $-\frac{y^3}{b} + cy \pm a_0 + w = 0$. By substituting $y = x$ into eq. (6) the characteristic equation about y becomes

$$\begin{aligned} F(\lambda) = {} & \lambda^3 + (b - a - c)\lambda^2 \\ & + \left(-ab - \frac{ay^2}{b} - cb + y^2 \right. \\ & \left. + ac \right)\lambda + acd - 3ay^2. \end{aligned} \tag{7}$$

When the parameters are satisfied:

$$FB : acb - 3ay^2 = 0. \tag{8}$$

The number of equilibria will change. At this time, fold bifurcation may occur, resulting in jumping phenomenon among different equilibria.

When the eigenvalue of the equilibrium point passes through the virtual axis, Hopf bifurcation may emerge. By calculating the eigenvalue of eq. (2), the following conditions need to be satisfied:

$$\begin{cases} (b - a - c)\left(-ab - \dfrac{ay^2}{b} - cb + y^2 + ac \right) \\ = acb - 3ay^2, \\ b - a - c > 0, \\ -ab - \dfrac{ay^2}{b} - cb + y^2 + ac > 0. \end{cases} \tag{9}$$

Then, there is a pair of pure virtual roots in characteristic eq. (7) and Hopf bifurcation can occur, leading to periodic oscillations.

4. Bursting oscillations and analysis of their mechanism

The fast subsystem not only determines the form of the quiescent states and spiking states of the system, but also resolves the transformation form between them. In this section, b is selected as the regulating parameter, and the fixed parameters are $A = 5, \Omega = 0.03, a = 2.5, c = 1.5, a_0 = -1$. Explore the evolution laws of the dynamic behaviours for system (2) when b takes different values. Next, two typical cases will be analysed to explain the oscillation phenomenon and its generation mechanism.

Case 1: $b = 0.5$

When $b = 0.5$, figures 1a–c show the phase portraits of system (3) on the (x, y), (z, y) and (x, z) planes, respectively. It can be seen that the phase portraits of system are symmetrical about x or y in each plane. As can be seen from figure 1d, the system has two spiking states $\mathrm{SP}_\pm$ and two quiescent states $\mathrm{QS}_\pm$ under this set of parameters. In addition, the direction of the system trajectory can be more accurately judged. With the passage of time, the amplitude of oscillations in the SPs showed an initial gradual increase and then a slow decrease. Moreover, the trajectory clearly crossed the non-smooth interface during the initial oscillations process, and then slowly detached its contact with the interface, basically keeping the oscillations in the smooth region. When the trajectory is contacted with the non-smooth interface again, the system will begin to proceed into the QSs, which means that the system has completed the oscillations in the first half period, and combined with its

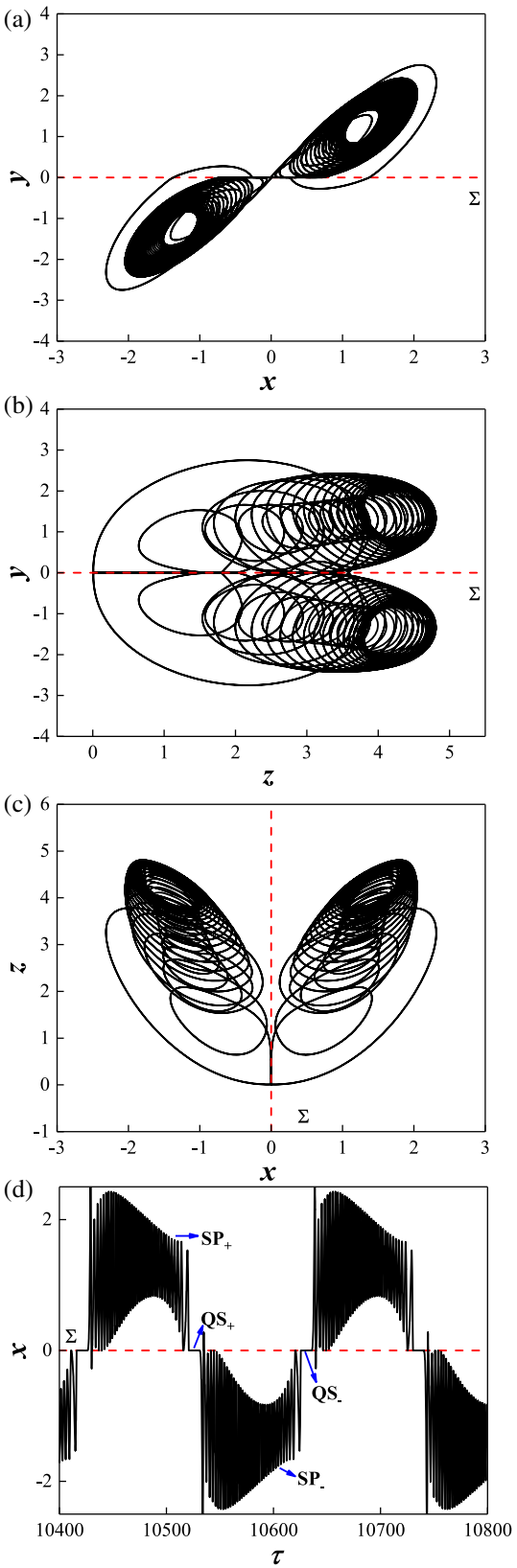

Figure 1. The bursting oscillations for $b = 0.5$. (**a**) Phase portrait on the (x, y) plane, (**b**) phase portrait on the (z, y) plane, (**c**) phase portrait on the (x, z) plane and (**d**) time history for x.

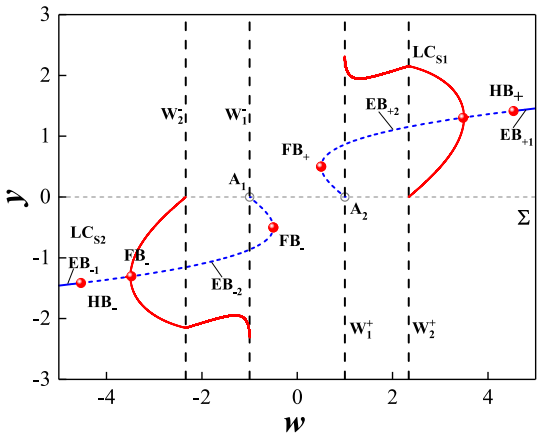

Figure 2. When $b = 0.5$, the superposition of equilibrium branch and bifurcation diagram on the (w, y) plane.

transformed phase portrait, it can be accurately judged that the trajectory oscillates in the counterclockwise direction as w increases (see figure 3a).

To further reveal the dynamic characteristics of the system, a superposition of the equilibrium curves, bifurcation figure and the envelope diagram of the limit cycle of the system under this set of parameters is given, as shown in figure 2.

In figure 2, the generalised autonomous system is divided into two smooth subsystems $F_{\pm}$ by the non-smooth interface Σ, and their corresponding equilibrium branches are denoted as $\mathrm{EB}_{\pm i}(i = 1, 2)$. The blue solid line $\mathrm{EB}_{\pm 1}$ represents stable equilibrium branches and blue short dashed line $\mathrm{EB}_{\pm 2}$ represents unstable equilibrium branches. $\mathrm{HB}_{\pm}$ denote two supercritical Hopf bifurcations, $\mathrm{FB}_{\pm}$ denote two fold bifurcations, while the red solid curves LC_{S1} and LC_{S2} denote the stable limit cycle resulting from the supercritical Hopf bifurcation HB_{+} and HB_{-}, respectively. The segment above the equilibrium branch corresponds to the maximum of the limit cycle amplitude and the segment below the equilibrium branch corresponds to the minimum of the limit cycle amplitude.

From the figure above, the general location of the disappearance and appearance of limit cycles LC_{S1} and LC_{S2} can be observed. By superposing with the equilibrium, the reason for the appearance and disappearance of the limit cycle can be analysed more clearly, and the dynamic properties of the system under this set of parameters can be explored. Next, the transformed phase portrait of (w, y) is superimposed with figure 2 again, and the system's bursting oscillation mechanism is described in detail (see figure 3b).

As shown in figure 3b, without loss of generality, it is assumed that the trajectory starts at $w = -5$.

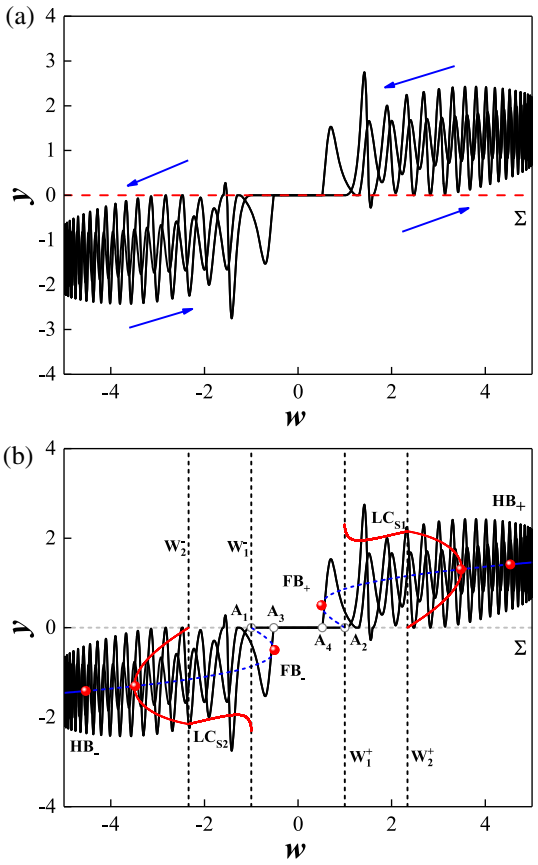

Figure 3. When $b = 0.5$, (**a**) the transformed phase portrait on the (w, y) plane and (**b**) the superposition of transformed phase portrait and figure 2.

The trajectory moves nearly along the stable equilibrium branch EB_{-1} within the smooth region D_-, when the trajectory reaches the first Hopf bifurcation point $HB_-(4.536, 1.414)$, the trajectory becomes unstable, at which point the system generated an unstable limit cycle LC_{S2} due to the emergence of supercritical Hopf bifurcation. At the same time, the oscillations of the trajectory gradually increases first and then gradually decreases with increasing w, and start to contact the non-smooth interface when the amplitude increases to a certain value. When the oscillations of the trajectory arrives at W_2^-, the upper half of the limit cycle LC_{S2} will reach W_1 along the non-smooth interface due to the generation of non-smooth bifurcation, that is, the occurrence of grazing-sliding bifurcation, and the lower half of the limit cycle will continue with the oscillations of the trajectory. When the trajectory reaches W_1^-, the limit cycle LC_{S2} disappears completely due to the emergence of non-smooth homoclinic bifurcation, and the saddle point on equilibrium branch EB_{-2} will also change to the junction equilibrium point on the non-smooth boundary by non-smooth transformations. Then, the trajectory will enter the non-smooth interface from point A_1. At this time, the system will enter the quiescent QS_- from the spiking SP_- and move along the non-smooth interface to point A_3. From here, it will break away from the quiescent QS_- and run along the unstable equilibrium branch EB_{+2} into the smooth area D_+. Its amplitude shows a trend of gradually increasing first and then slowly decreasing. As w increases, the homotopic character of the limit cycle LC_{S1} weakens, and the trajectory oscillations begins to show a relatively dense tendency, as well as shrinks and oscillates with limit cycle LC_{S1} towards the equilibrium branch EB_{+1} which produces the stable ultimate ring LC_{S1} when it goes through the supercritical Hopf bifurcation point $HB_+(-4.536, -1.414)$. When the trajectory branch reaches W_2^+, the limit cycle starts to contact the non-smooth interface surface, at which point the lower half of the limit cycle disappears due to the generation of grazing-sliding bifurcation. From point W_2^+ to point W_1^+, with the emergence of crossing-sliding bifurcation and non-smooth homoclinic bifurcation, the upper half of the limit cycle also completely disappears at point W_2^+. The trajectory will then proceed along the unstable equilibrium branch EB_{+2} from point A_2 to the non-smooth interface, the system also changes from the spiking state SP_+ to the quiescent state QS_+, which oscillates again in the smooth region D_- when the trajectory moves to A_4 and QS ends. Similar to its oscillations mode in area D_+, the amplitude of the trajectory first gradually increases to the highest point, then decreases slowly, and oscillates gradually away from the interface along the unstable equilibrium branch EB_{-2}. When the trajectory reaches the point $w = -5$, the oscillations end, that is, one period of oscillations is completed.

During this period of oscillations, the trajectory exhibited two spiking states $SP_\pm$ and two quiescent states $QS_\pm$. Moreover, the structure of the spiking states changed continuously with the oscillations of the limit cycle, which was accompanied by the generation of grazing-sliding bifurcation and crossing-sliding bifurcation.

To better explain the crossing-sliding bifurcation and grazing-sliding bifurcation in the spiking states, numerical simulations are carried out, and the (z, y) phase portraits and (y, t) phase portraits when $w = 1$ and $w = 2$ are given respectively.

Figures 4a and 4b present the phase portrait and their time history on the (z, y) plane of the system when $w = 1$. From figures 4c and 4d, we can see that when w is taken for different sets of parameters, there is a great difference in the sliding time at the non-smooth interface $y = 0$, and there is a similarity of a sticky sliding process. The difference is that

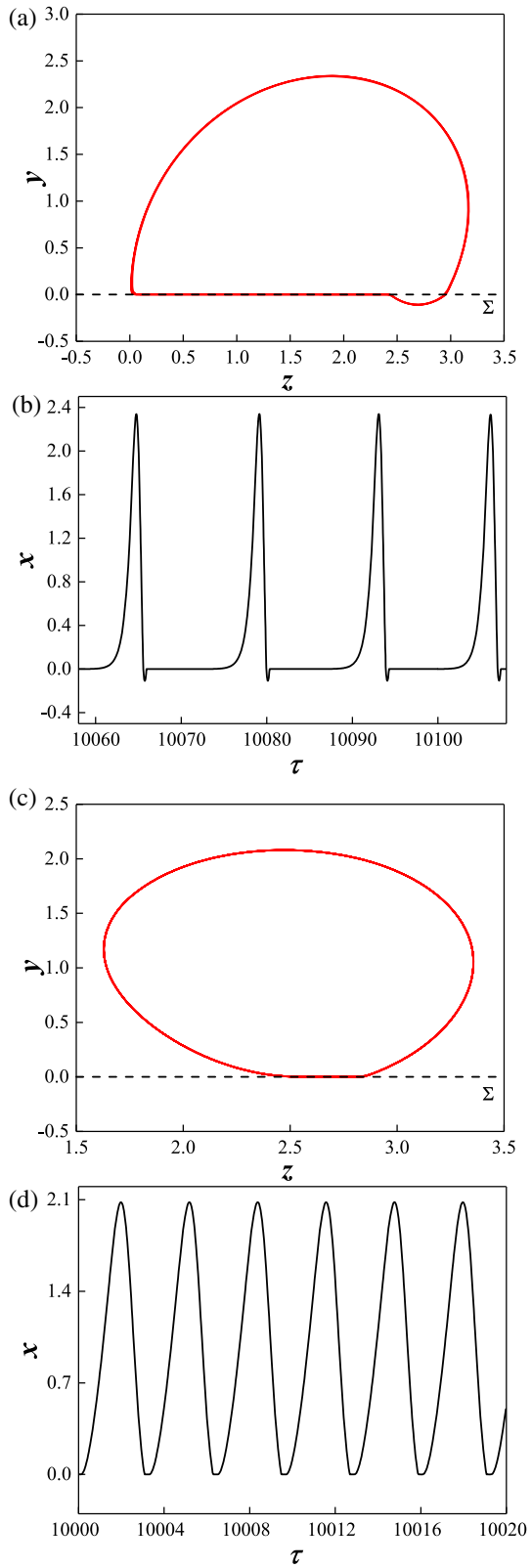

Figure 4. (**a**) Phase portrait on the (z, y) plane for $w = 1$, (**b**) time history for $w = 1$, (**c**) phase portrait on the (z, y) plane for $w = 2$ and (**d**) time history for $w = 2$.

as z continues to change, when $w = 1$, the trajectory begins to cross the non-smooth interface and then into D_- when $z = 2.5$ and back into the smooth region D_+ when $z = 3.0$. This process not only includes the sticky sliding process, but also is accompanied by the emergence of crossing-sliding bifurcation. From its time history diagram, it can be seen that the time of crossing the interface is particularly short compared with the time of sticky sliding. When $w = 2$, the trajectory moves with increasing z completely in the smooth region D_+. In addition, there is a distance of sliding on the non-smooth interface $y = 0$, that is, the sticky sliding process mentioned above. Compared with the former case, its sliding time on the interface is much shorter, its oscillations frequency increases, and the time each oscillation experiences gradually increases. This also verifies that the oscillations of trajectory will have a relatively dense trend with the weakening of the characteristics of homoclinic cycle, and the above process shows a critical case of crossing-sliding bifurcation.

Case 2: $b = 1.5$

In fact, with the change of parameter b, the form of bursting oscillations of the system is also changing. Next, $b = 1.5$ is selected and the other parameters remain unchanged to observe the dynamic behaviours of the trajectory in this case.

By observing figures 5a–5d and comparing with Case 1, it can be seen that the symmetry of oscillations is still unchanged, but the dynamic behaviours on the non-smooth interface has changed greatly. Comparing the phase portraits of (x, z) and (z, y) under the two groups of parameters, it can be found that the movement time of the trajectory on the interface $x = 0$ is much shorter, but the contact times with the interface $y = 0$ are more. In addition, it can be seen from its time history diagram that the oscillation amplitude of the trajectory increases first and then decreases in the process of back and forth oscillations. In order to reveal its bursting oscillations mechanism, its transformed phase portrait and equilibrium branch diagram are superimposed as shown in figure 6.

Through numerical simulation, it is found that the oscillations in this case experience only fold bifurcation. To explore the influence of the bifurcation on the bursting oscillations, $b = 1.5$ and other parameter values are substituted into eq. (6), when $y = -1.5$, and calculate the corresponding characteristic equation as follows:

$$f(\lambda) = \lambda^3 - 2.5\lambda^2 - 3.75\lambda - 11.25. \tag{10}$$

The characteristic roots are $\lambda_1 = 4.0896$, $\lambda_{2,3} = \pm 0.7948i \pm 1.4557$. When the eigenvalues of the sys-

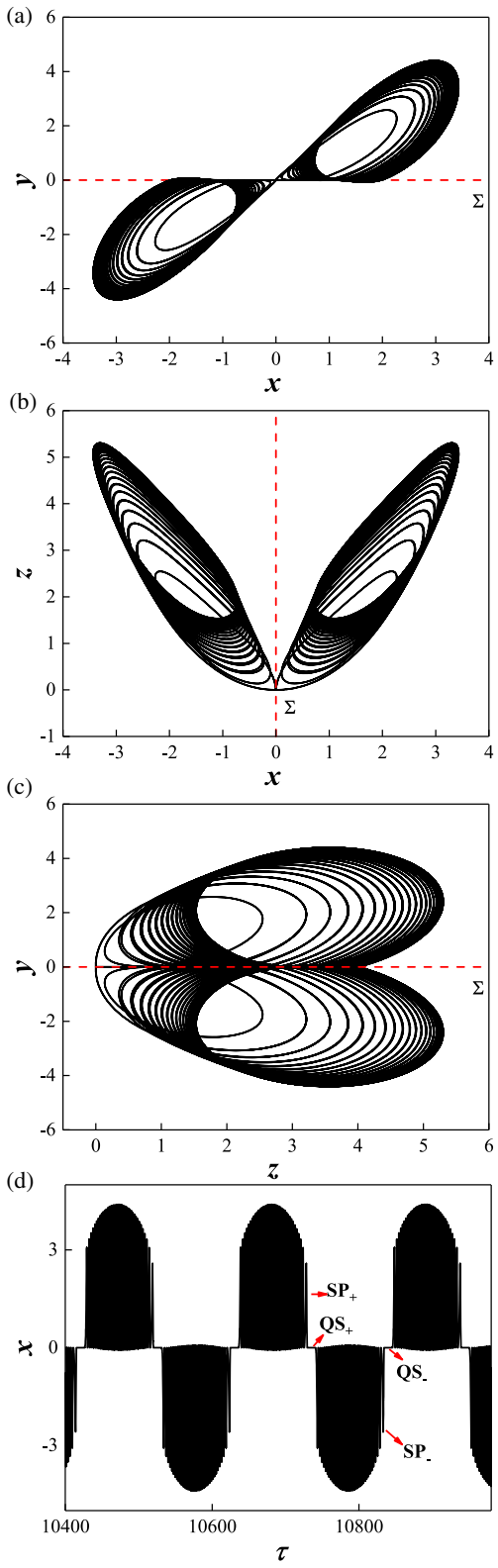

Figure 5. Bursting oscillations for $b = 1.5$. (**a**) Phase portrait on the (x, y) plane, (**b**) phase portrait on the (x, z) plane, (**c**) phase portrait on the (z, y) plane and (**d**) time history for x.

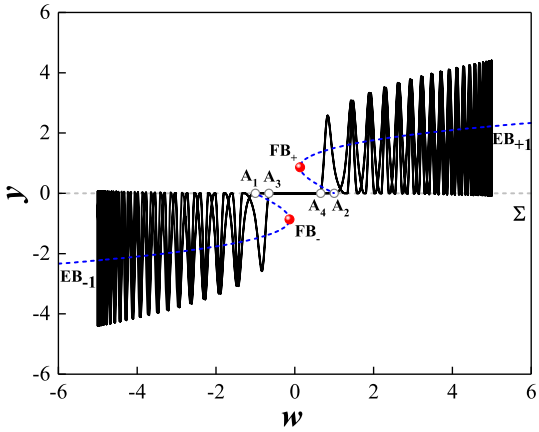

Figure 6. When $b = 1.5$, the superposition of transformed phase portrait on the (w, y) plane and equilibrium branch.

tem contain negative real parts, the equilibrium branch is stable, and so the equilibrium branch of the system is unstable. Therefore, it can be deduced that bursting under this group of parameters is not fold/fold bursting. Looking at figure 6, it is assumed that the trajectory starts from $w = -5$ and moves along the unstable equilibrium branch EB_{-1} to the first fold bifurcation point FB_-. Because the fold bifurcation does not affect the stability of the equilibrium branch, the trajectory will continue to move along EB_{-1} to point A_1, end the operation in the smooth region D_- and enter the QSs from the SPs. It moves along the non-smooth interface to point A_4 and enters the smooth region D_-. Then, it runs along the unstable equilibrium branch EB_{+1} until it reaches the point $w = 5$, the trajectory starts to turn around, passes through FB_+ along curve EB_{+1}, reaches point A_2, ends the SPs and enters the QSs. After that, it starts to reach A_3, along the non-smooth interface, enters the region D_- again, continues to run along the equilibrium branch EB_{-1}, and finally arrives at the point $w = 5$ to complete a period of oscillations.

In the process of oscillations, although Hopf bifurcation does not occur, the limit cycle still appears because the system itself has a limit cycle branched from the saddle point homoclinic orbit [31]. With the continuous change of slowly varying parameters, the structure of the trajectory in the spiking states also changes partially. With the increasing amplitude, the oscillations of the trajectory always run close to the non-smooth interface, and the minimum or maximum amplitude is always maintained at $y \approx 0$. When the slowly varying parameter $w = 1.5$, the amplitude in the y-axis and its minimum point (x, y, z) satisfy

$$\dot{y}|_{y'=0} = -x'z' + cy' + a_0 + 1.5 = 0. \tag{11}$$

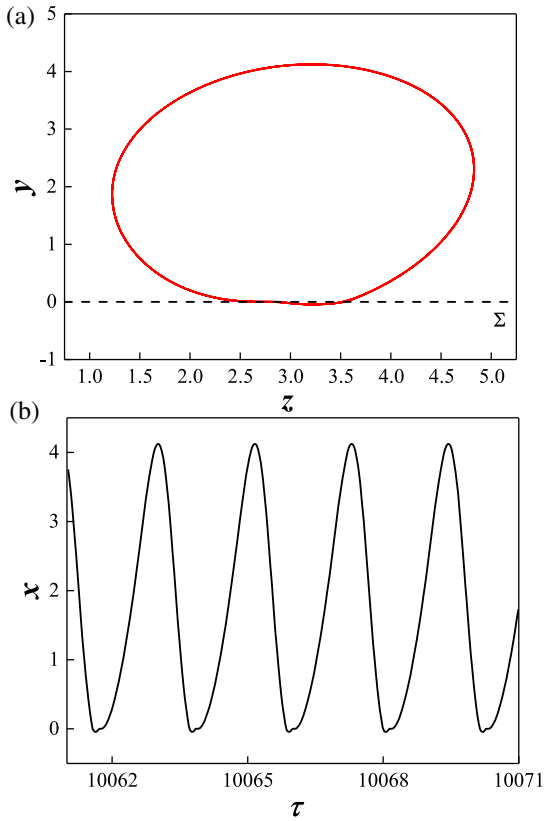

Figure 7. (**a**) Phase portrait on the (z, y) plane for $w = 4$ and (**b**) time history for $w = 4$.

This indicates that the trajectory always runs tangent to the non-smooth interface during oscillations. When the slowly varying parameter exceeds $w = 1.5$, it starts to run to the smooth region D_+ which indicates that the trajectory will enter the sliding region $\Sigma_s = \{(x, z)|y = 0\}$ when it runs counterclockwise and returns to the interface again. Therefore, the slowly varying parameter $w = 1.5$ corresponds to the unconventional bifurcation, called the grazing-sliding bifurcation, of the generalised autonomous system (3). When the slowly varying parameter $w = 4$, the oscillation mode of crossing-sliding begins to appear when the trajectory contacts the non-smooth interface. It will oscillate into region D_- and then return to the non-smooth interface for sliding. Therefore, the differential equation is numerically simulated as

$$\dot{y} = -xz + cy + a_0 + 4. \tag{12}$$

The phase diagram and time history diagram of the corresponding trajectory in the (y, z) plane are shown in figure 7.

Combined with the previous numerical calculation, it can be inferred that the bifurcation at this time is still grazing-sliding bifurcation, but the trajectory stays at the interface for a short time during the oscillations process due to the slow passage effect [32].

5. Conclusion

Taking Lü system as an example, this paper focusses on the mixed-mode oscillations and its generation mechanism of non-smooth system with two time scales. By comparing the above two groups of phenomena, it can be seen that the non-smooth transformation of the equilibrium point leads to the mutual transition between the SPs and the QSs of the system during bursting oscillations. In addition, due to the existence of non-smooth term, the structure of SPs also change with the change of slowly varying parameters in the process of bursting oscillations of the trajectory, which may produce non-smooth bifurcation, such as grazing-sliding bifurcation and crossing-sliding bifurcation. Therefore, when exploring the dynamic behaviours of non-smooth system under periodic excitation, not only the influence of Hopf bifurcation and fold bifurcation on bursting oscillations, but also the possible bifurcation of the trajectory at non-smooth interface should be considered. By superimposing the equilibrium branch, bifurcation diagram and transformed phase portrait, the bursting oscillation mechanism of the trajectory in one period are described, which provides a good method to explore the bursting oscillations mechanism of non-smooth system under different scale effects.

Acknowledgements

The author is thankful to editors and referees for the careful reading and valuable suggestions that improve the quality and description of this manuscript. This work was supported by National Natural Science Foundation of China (Grant No. 12102148) and Natural Science Research of Jiangsu Higher Education Institutions of China (Grant No. 21KJB110010).

References

[1] H N Li, S Y Xiao and S Y Wang, *ASME PVP* **2**, 445 (2002)
[2] W Ahmed, A Maqsood and R Riaz, *Results Phys.* **8** (2018)
[3] J Y Hou, X H Li, D W Zuo and Y N Li, *Eur. Phys. J. Plus* **6**, 132 (2017)
[4] Y Wang and J E Rubin, *J. Comput. Neurosci.* **3**, 41 (2016)
[5] D M Blitz, A E Pritchard, J K Latimer and A T Wakefield, *J. Exp. Biol.* **7**, 220 (2017)

[6] E Vitale, D Deneele, M Paris and G Russo, *Appl. Clay Sci.* **141**, 36 (2017)
[7] L Cuevas, D Nei and C Manzie, *Int. J. Robust Nonlinear Control* **30**, 14 (2020)
[8] M Peng, Z D Zhang, Z F Qu and Q S Bi, *Pramana – J. Phys.* **94**, 14 (2020)
[9] W H Mao, Z D Zhang and S Z Zhang, *Chin. J. Theor. Appl. Mech.* **53**, 3 (2021)
[10] A L Hodgkin and A F Huxley, *The J. Physiol.* **4**, 117 (1952)
[11] F Verhulst, *Nonlinear Dyn.* **4**, 50 (2007)
[12] A Haselbacher, F M Najjar, L Massa and R D Moser, *J. Comput. Phys.* **2**, 229 (2010)
[13] E M Izhikevich, *Int. J. Bifurc. Chaos* **6**, 10 (2000)
[14] J Rinzel, *Bull. Math. Biol.* **1**, 52 (1990)
[15] A Lerchner and J Rinzel, *Neurocomputing* **65**, 777 (2005)
[16] M Brøns, M Desroches and M Krupa, *Math. Popul. Studies* **2**, 22 (2015)
[17] Z D Zhang, Y Y Li and Q S Bi, *Phys. Lett. A* **377**, 975 (2013)
[18] Y Q Xing, X K Chen, Z D Zhang and Q S Bi, *Acta Phys. Sinica* **9**, 65 (2016)
[19] H J Xu, Z D Zhang and M Peng, *Nonlinear Dyn.* **108**, 2 (2022)
[20] K Zimmermann, I Zeidis and V Lysenko, *Appl. Math. Model.* **89**, 13 (2021)
[21] B Y Shen and Z D Zhang, *Pramana – J. Phys.* **95**, 97 (2021)
[22] Y F Lv, R Yuan and Y Z Pei, *J. Comput. Appl. Math.* **250** (2013)
[23] A A Transeth, R I Leine, C Glocker and K Y Pettersen, *IEEE Trans. Robotics* **2**, 24 (2008)
[24] F Angulo, G Olivar, G A Osorio, C M Escobar, J D Ferreira and J M Redondo, *Commun. Nonlinear Sci. Numer. Simul.* **12**, 17 (2012)
[25] J A Amador, G Olivar and F Angulo, *Diff. Equ. Dyn. Syst.* **21**, 173 (2013)
[26] G R Chen and J H Lv, *Lorenz systems family dynamic analysis of control and synchronization* (Science Press, Beijing) (in Chinese)
[27] M Aqeel, A Azam and S Ahmad, *Eur. Phys. J. Plus* **10**, 132 (2017)
[28] L Qiang, N Benyamin and L Feng, *Chaos Solitons Fractals* **114**, 230 (2018)
[29] B Yan, S B He and S J Wang, *Math. Prob. Eng.* **2468134**, 1 (2020)
[30] M L Ma , L W Xiong, Z Y Shu, Y J Fang and M J Wang, *Int. J. Bifurc. Chaos* **13**, 31 (2021)
[31] R Zhang, M Peng, Z D Zhang and Q S Bi, *Chin. Phys. B* **11**, 27 (2018)
[32] L Holden and T Erneux, *SIAM J. Appl. Math.* **4**, 53 (1993)